Segmentation of Sedimentary Grain in Electron Microscopy Image

Aleš KŘUPKA [1], Kamil ŘÍHA [1], Lenka KŘÍŽOVÁ [2]

[1] Dept. of Telecommunications, Brno University of Technology, Technická 12, 612 00 Brno, Czech Republic
[2] Dept. of Physical Geography and Geoecology, Charles University in Prague, Albertov 6, 128 43 Praha 2, Czech Republic

akrupka@phd.feec.vutbr.cz, rihak@feec.vutbr.cz, krizova@natur.cuni.cz

Abstract. *This paper describes a novel method developed for the segmentation of sedimentary grains in electron microscopy images. The algorithm utilizes the approach of region splitting and merging. In the splitting stage, the marker-based watershed segmentation is used. In the merging phase, the typical characteristics of grains in electron microscopy images are exploited for proposing special metrics, which are then used during the merging stage to obtain correct grain segmentation. The metrics are based on the typical intensity changes on the grain borders and the compact shape of grains. The experimental part describes the optimal setting of parameter in the splitting stage and the overall results of the proposed algorithm tested on available database of grains. The results show that the proposed technique fulfills the requirements of its intended application.*

Keywords

Image segmentation, sedimentary grains, split-and-merge, watershed, gradient, markers.

1. Introduction

The segmentation of unlithified sedimentary grains in electron microscopy images is a basic operation in the computer automated geomorphologic analysis. This analysis is a part of the time consuming geomorphologic method called exoscopy. Exoscopy includes the extraction and analysis of various structure characteristics from surface of examined grains. An electron microscope is used because of the small grains sizes. The grains are cleaned using concentrated HCl and stuck to a graphite tape. Then each separated grain is focused and its detailed digital image is obtained. Examples of grain images can be seen in Fig. 1. After the grains have been captured, the images are examined and various structural forms are searched for on the surface of grains, statistics of their occurrences are collected [1]. Especially this part of exoscopy is a very time consuming task, which is done manually by trained and experienced experts. For this reason the potentials of computer aided analysis using modern image processing techniques are being investigated, which would automate or significantly shorten the work of exoscopy experts.
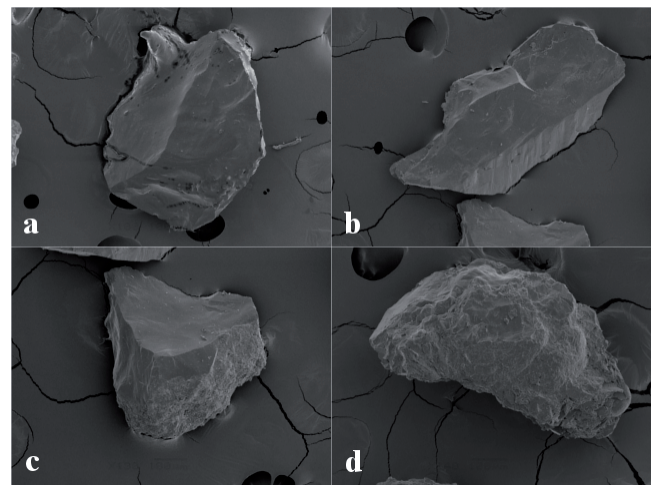

Fig. 1. Examples of sedimentary grain captured by electron microscope

The segmentation of sedimentary grains includes the selection of pixels in the image, which belongs to the analyzed grains, and so the region of interest can be separated from the background. Generally, image segmentation is an essential step in the procedures of computer vision, which is also true in the analysis of sedimentary grains, where the best possible selection of grain pixels is needed. Image segmentation is a wide field of image signal processing, where a variety of methods have been developed.

Regarded as the fundamental and simplest segmentation technique can be thresholding, which assigns pixels to defined classes according to its values of intensity; for each class a range of intensity values is defined. Different methods for optimal threshold selection exist [2], [3], [4]. When using thresholding for sedimentary grain segmentation, there are problems caused by overlapping intensity values inside and outside of the grain, especially when the surface of grains is smooth and thus similar to the background, see Fig. 1a, which makes thresholding not suitable for this purpose.

Another segmentation approach is based on edge detection. It assumes that objects in an image have clear borders, where also a significant change of intensity is present.

Canny's edge detection [5] or edge relaxation method [6] can be mentioned among the sophisticated methods. Edge detection itself is not a result of segmentation, so further steps are required. It is assumed that the object boundary is represented by a closed edge called contour. In the case of sedimentary grains, it is nontrivial to find the resulting contour because of the presence of many spurious edges caused by artifacts in the background or diverse relief of the grain, see Fig. 1c, d.

A well-known method, widely used in many present segmentation tasks, is the watershed-based segmentation [7], [8], [9], where segmentation is considered as a process of relief flooding. The gradient magnitude of original image is usually used as the relief, where ridges in the relief usually represent object boundaries. In the relief, positions are found that are called regional minima which are used as initialization points of flooding. The number of these initialization points determines the number of segments in the image. The area of relief which is flooded by water from one regional minimum is called the catchment basin. As the flooding process progresses, the catchment basins are extended until different catchment basins meet together. The boundaries between the catchment basins are called watersheds and represent the borders of resulting segments. The usual drawback of watershed segmentation is splitting into many small regions as a result of the big number of regional minima in the relief image. This phenomenon is known as oversegmentation and various methods have been developed to cope with it.

One possible approach is to adjust the gradient image before applying the watershed segmentation. For this purpose, the marker-based watershed segmentation was proposed [10], where regional minima are eliminated, using morphological reconstruction, except positions determined by markers, so the number of markers gives the number of resulting segments and therefore oversegmentation can be avoided. The main point is the definition of markers. In cases of semiautomatic segmentation, the markers are specified by the human operator and then watershed segmentation is performed. When automatic marker determination is needed, prior specific information about the processed images is used. This prior information about shape and position is used in [11] for creating a statistical atlas, which helps to locate the markers and thus to alleviate oversegmentation. However, the use of the atlas is restricted to well-defined segment shapes. In [12], oversegmentation is addressed using the principle of resolution pyramids. It is assumed, that the most significant components are identified in both higher and lower image resolution. The information from different resolutions is then utilized for final marker determination, and watershed segmentation is applied. After that, regions with similar mean pixel intensity can be additionally merged.

Generally, region merging techniques are very often used when dealing with watershed oversegmentation, and so after watershed splitting, regions are merged together to create meaningful objects. Adjacent regions are being merged as long as the resulting merged region fulfills some defined homogeneity criterion [13], [14], [15]. The adjacency between regions is often logically represented by the Region Adjacency Graph [16], where nodes of graph stand for regions and edges present their common borders. Weights are usually assigned to edges as a measure of dissimilarity between regions. These weights then influence the process of merging. In [17] a general technique of graph merging is proposed, where two regions are merged if they form a specific couple in terms of defined dissimilarity criterion based on the mean intensity of region. In [18] the topographic relief of a region is fitted by a plane using the least square fitting, the difference between the plane parameters of adjacent planes is then used as a dissimilarity criterion. The merging rules can also be based on a criterion specific to a given application, [19] introduces a measure of rectangularity for the segmentation of houses in remote sensing imagery; however, initial region classification into foreground or background is needed. In [20], more images of marble sections are captured with different polarization settings, which enhances the information about marble grains, so the specific merging criterion can be stated. The proposal in [21] is based on the known shape of segmented object and thus the most promising part in the oversegmented image is chosen. It is also possible to extract texture features from particular watershed segments and then classify them using machine learning techniques similarly as to [22].

No automatic segmentation technique has been published, which would determine the area of sedimentary grain in electron microscopy images. Despite the existence of segmentation methods in the field of geology [23], [24], [25], the characteristics of images, that these methods were made for, are totally different from sedimentary grains and thus these methods are not suitable for our purposes. In the field of electron microscopy, several works dealing with segmentation have been published, but the techniques developed were intended for the application of segmentation of cells in electron tomography images [26], [27], whose nature is also different from the images capturing sedimentary grains. Thus the development of a new method performing sedimentary grain segmentation was needed. Because of the nature of the images, watershed segmentation was chosen as the appropriate basic segmentation tool.

However, when applying the watershed transform to sedimentary grains, oversegmentation is very strong. This can be reduced by using a method from [10], when Gaussian blur is applied to a relief image, which is then thresholded to obtain marker positions. Nevertheless, this operation does not resolve oversegmentation completely. Because of the miscellaneous shapes of grains, no prior information can be used for more accurate marker setting. Therefore, to obtain a final grain segment, particular regions need to be additionally merged, and so the region merge scheme is used. The published methods of watershed region merging present either the general way of

region merging, which is not sufficient for sedimentary grain segmentation, or they are developed for a specific segmentation problem, where its inherent characteristics are used to specify the merging criterion and merging procedure. However, these rules are not applicable to grain segmentation. For example, the merging criterion based on intensity or texture properties is not suitable because different parts of a grain can have different mean intensity values as well as totally different type of texture, see Fig. 1. Also, only one image is available to one grain so no other modality can be used to enhance the information for segmentation. This paper thus presents a proposal of a new method for sedimentary grain segmentation, which takes into account the typical characteristics of grains. The method is presented in the following text.

2. Description of Segmentation Method

The procedure of the proposed method can be seen in Fig. 2. For region splitting, the marker-controlled watershed segmentation is used. Markers are obtained as connected components of a thresholded gradient image. The image split into regions is described by the Region Adjacency Graph [16] and then the regions are merged to obtain a segment of the grain, using specially proposed rules. Individual parts of the procedure are described in detail in the following text.

2.1 Splitting Stage

As mentioned previously, the magnitude of original image gradient is used as the input of watershed segmentation. A gradient image can be computed by applying various linear filters. In our case, filters in the form of the 1st derivative of the Gaussian function are used. Direction α is the parameter of these filters; it steers the angle of their rotation, and thus these filters are referred to as steerable filters [28]. Examples of filters for different directions α can be seen in Fig. 3. When an image is filtered using a steerable filter with direction α, then the resulting image

Fig. 2. Procedure of proposed method.

is denoted by $grd_\alpha(x,y)$. The reason for using steerable filters is to highlight important intensity changes in a given direction α while suppressing insignificant chaotic changes caused by texture or noise. The input of watershed segmentation is a gradient magnitude image representing the relief given as

$$grd_{abs}(x,y) = \left|grd_0(x,y)\right| + \left|grd_{90}(x,y)\right| \qquad (1)$$

which is the sum of absolute values of the images filtered by steerable filters in mutually perpendicular directions; the resulting image $grd_{abs}(x,y)$ can be seen in Fig. 4b.
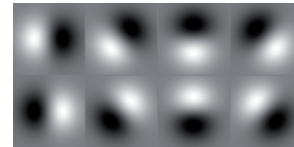

Fig. 3. Examples of steerable filters in directions $\alpha \in \{0, 45, 90, 135, 180, 225, 270, 315\}$ °

A direct application of the watershed transform would yield an oversegmented image, thus the markers are extracted first. The image $grd_{abs}(x,y)$ is processed using thresholding with threshold t_{mark}, then the connected components are used as markers, see Fig. 4c. An optimal selection of the t_{mark} value is presented in Section 3. Marker-controlled watershed segmentation is then performed, which results in an image split into regions, see Fig. 4d.

2.2 RAG Evaluation

Images of sedimentary grains have some specific characteristics which are used for segmentation. The most important is the character of the intensity gradient on the grain border. In the background-grain direction, the intensity changes mostly from the low (black) to the high level (white). For the evaluation of the gradient, the original images are processed by steerable filters shown in Fig. 3. Gradient images are obtained for particular directions α, see Fig. 5 with the results describing the image gradient in a given direction. As can be seen in Fig. 5, a pixel on the grain border is always of the lowest negative $grd_\alpha(x,y)$ value for such a direction α, that is perpendicular to the grain edge direction and is oriented from background to grain. In the course of determining the direction of α, only the 8-neighborhood of a given pixel is considered. Thus, the value of α is selected only from 8 directions $\alpha \in \{0, 45, 90, 135, 180, 225, 270, 315\}°$. In an image position where the assumption of intensity change from lower to higher value is fulfilled, the grain edge appearance can be expected. This presumption is used as a rule in the process of region merging where the sum of gradient values $grd_\alpha(x,y)$ along a potential grain border is computed, the value of α for a given position is always chosen as the perpendicular direction to a potential grain border. The lower the resulting sum along the border of a given region set, the bigger the probability that this set of regions corresponds to a grain segment.
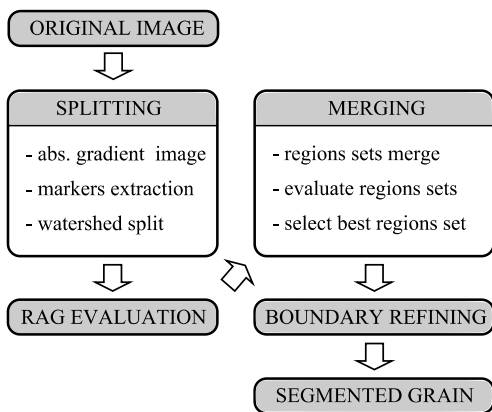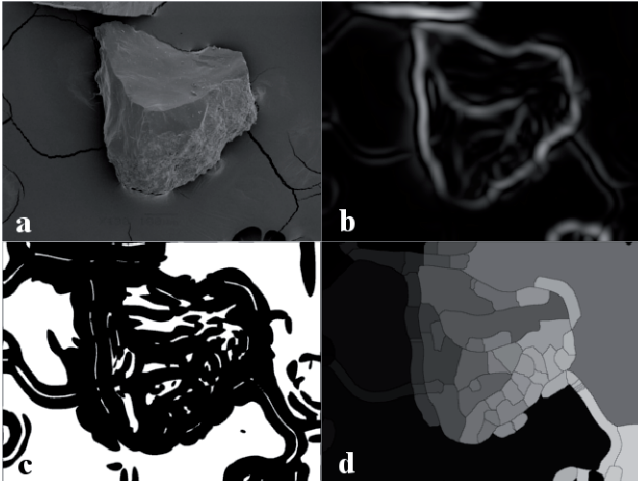
Fig. 4. Procedure of watershed splitting. (a) Original image. (b) $grd_{abs}(x,y)$ image. (c) Marker image. (d) Image split into regions.
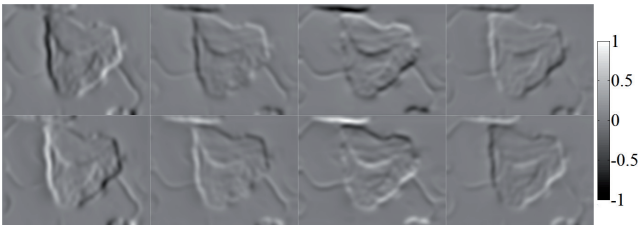

Fig. 5. Resulting images filtered by steerable filters in directions $\alpha \in \{0, 45, 90, 135, 180, 225, 270, 315\}$.

The image split into labeled regions can be interpreted using the Region Adjacency Graph (RAG) and in this form, it can be used as the input for the procedure of finding the regions belonging to the grain. The regions in the image are represented by graph nodes, the borders between the regions are represented by graph edges, see Fig. 6.
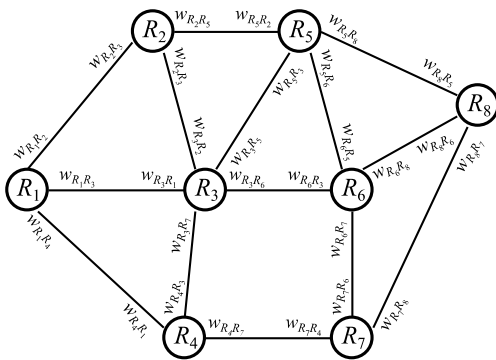

Fig. 6. Region Adjacency Graph.

As can be seen from RAG, the number of edges connected to the node of region R_i represents the number of regions which share an adjacent border with region R_i. A set of coordinates of pixels on the border between the regions R_i and R_j are denoted by $(x,y) = a_{R_iR_j}(p)$, where $p = 1,2,\dots N_{R_iR_j}$ is the pixel index and $N_{R_iR_j}$ is the number of pixels of adjacent border. Direction α, which is perpendicular to the edge tangent for a given border pixel p which

is oriented to region R_i is denoted by $\alpha = b_{R_iR_j}(p)$. The weight $w_{R_iR_j}$ is then assigned to the edge oriented from node R_i to R_j according to the relation

$$w_{R_iR_j} = \frac{\sum_{p=1}^{N_{R_iR_j}} grd_{b_{R_iR_j}(p)}(a_{R_iR_j}(p))}{N_{R_iR_j}}. \tag{2}$$

The value of $w_{R_iR_j}$ then represents the average value of $grd_\alpha(x,y)$ along the edge between regions R_i and R_j in a given direction $b_{R_iR_j}(p)$ for every pixel. This way the edges of RAG are evaluated.

2.3 Merging Stage

After the borders between adjacent regions have been evaluated, region merging is performed. The goal is to obtain a set of regions whose union forms the segment determining the grain area. Region merging is done in consecutive steps; in every step a new region is appended to the current set of merged regions. When the total number of regions in the image is K, then merging is performed in K steps. A current set of k regions representing a segment after k steps of merging ($k = 1,2,\dots,K$) where the initial region was R_i is denoted by R_{ik}. The current set of regions after the k-th step of merging thus consists of the previous set of regions $R_{i(k-1)}$ and a new region R_j. After the merging procedure, K sets of regions R_{ik} are available. Since the initial region R_i, where the merging should start, is not known, the whole merging procedure is repeated for all variants of the initial region R_i ($i = 1,2,\dots,K$). The best set of regions then has to be chosen according to the defined metrics in the next section. During the procedure of merging the order is essential in which in every step a new region R_j is appended to the previous set $R_{i(k-1)}$. The union of the set of regions R_{ik} merged in the k-th step represents the current segment, whose neighboring regions form a set denoted by V_{ik}. In the $(k+1)$-th step, the region R_j from a set of regions V_{ik} is appended to the set of regions R_{ik} according to the following rule

$$w_{R_{ik}R_j} = \max_{R_m \in V_{ik}} w_{R_{ik}R_m}, \tag{3}$$

i.e. from the current neighboring set V_{ik} such a region R_j is chosen where the edge in RAG oriented from R_{ik} to R_j has the maximal weight. This rule is based on the assumption stated in Section 2.2, where the border pixels of a grain in the image $grd_\alpha(x, y)$ have relatively low negative values in a correctly selected direction α. When the union of a set R_{ik} represents a correct segment of grain area, the weights of edges oriented from the set of regions R_{ik} to the neighboring set of regions V_{ik} have also low negative values. During the merging procedure, it is thus desirable to move toward a low average of edge weights of the current set R_{ik}, which is done by eliminating the maximal edge weights using rule (3). This way, the borders of regions with low negative

weights are preserved for the maximal number of merging steps.

2.4 Regions Sets Evaluation

After region merging, it is necessary to select the best set of regions R_{ik} (it means to find out specific values of i and k). To discover the most promising set R_{ik}, the following metrics, which describe particular sets R_{ik}, were proposed. The first metric represents the average weight of the graph edges connected to a set of regions R_{ik}.

$$m_{R_{ik}} = \frac{\sum\limits_{R_j \in V_{ik}} w_{R_{ik}R_j} N_{R_{ik}R_j}}{\sum\limits_{R_j \in V_{ik}} N_{R_{ik}R_j}} \quad (4)$$

where $N_{R_{ik}R_j}$ is the number of pixels on the common border between set of regions R_{ik} and region R_j. This metric should have a minimal value for the set of regions R_{ik} corresponding to the correct grain segment. The next metric is the standard deviation of weights belonging to edges oriented from a set of regions R_{ik} to regions from set V_{ik}; it is defined as

$$s_{R_{ik}} = \operatorname*{stddev}_{R_j \in V_{ik}} (w_{R_{ik}R_j}) \cdot$$

This metric should have a minimal value for the set of regions R_{ik} corresponding to the correct grain segment. The third metric uses the ratio of area of current segment R_{ik} to its perimeter. This ratio grows linearly with the area, thus this ratio is normalized by the ratio of circle area to its perimeter r, where the circle area is equal to the area of currently evaluated segment R_{ik}. Let the area of region R_j be denoted by F_{R_j}, then the third metric is

$$c_{R_{ik}} = \frac{\dfrac{\sum\limits_{R_j \in R_{ik}} F_{R_j}}{\sum\limits_{R_j \in V_{ik}} N_{R_{ik}R_j}}}{\dfrac{\pi r^2}{2\pi r}} = \frac{2\sqrt{\pi \sum\limits_{R_j \in R_{ik}} F_{R_j}}}{\sum\limits_{R_j \in V_{ik}} N_{R_{ik}R_j}} \quad (5)$$

where the circle perimeter was substituted by

$$r = \sqrt{\frac{\sum\limits_{R_j \in R_{ik}} F_{R_j}}{\pi}} \cdot$$

The maximal ratio of area to perimeter is given for the case of circle, which implies that the maximal value of metric $c_{R_{ik}}$ is equal to 1, which is fulfilled in the case of the current circular segment R_{ik}. The grains are of compact shapes, thus the set of regions R_{ik} corresponding to the grain segment should have a higher value of this metric than the other sets of regions R_{ik}.

As stated in Section 2.3, the merging process is repeated K times and every time it is initialized with a different region R_i. The resulting number of sets of regions is thus K^2. The obtained sets of regions R_{ik} can be evaluated by the previously introduced metrics. Because $i = 1,2,\ldots,K$, and $k = 1,2,\ldots,K$, the metric values can be formed into matrices for better visual interpretation. Therefore, matrices $\mathbf{M}(i,k) = m_{R_{ik}}$, $\mathbf{S}(i,k) = s_{R_{ik}}$ a $\mathbf{C}(i,k) = c_{R_{ik}}$ are created, their visualization for the grain in Fig. 4 is shown in Fig. 7a,b,c. Obviously, some characteristic sets of regions R_{ik} corresponding to the segment of the grain can be chosen. These sets are represented by low values in matrices $\mathbf{M}$ and $\mathbf{S}$, and by high values in matrix $\mathbf{C}$. It can be seen that other sets of regions R_{ik} exist which do not correspond to the grain segment but have a potentially promising value of the defined metrics, see the last columns of matrices in Fig. 7a,b,c. The choice of a correct set of regions R_{ik} is maximized by the algorithm using the described metrics and addition constraints, which will be described in the next section.

2.5 Selection of Best Set of Regions

The selection of the best set of regions R_{ik} is performed in two steps. In the first step, such sets of regions R_{ik} are removed, which are out of the following bounds:

- The set R_{ik} has a lower number of pixels than the defined threshold (i.e. minimal area of segment).

- The set R_{ik} contains holes (i.e. some regions inside the segment consisting of the set R_{ik} do not belong to the set R_{ik}).

- The metric $c_{R_{ik}}$ of R_{ik} is of higher value than 1.

- The metric $m_{R_{ik}}$ of R_{ik} is of higher value than 0.

The R_{ik} sets with holes are removed to prevent the metrics used being distorted by inner borders with non-merged region. The sets R_{ik} with the metric $c_{R_{ik}}$ higher than 1 are discarded because compact shapes cannot have this metric higher than 1. When the metric $c_{R_{ik}}$ is higher than 1, then it is caused by merging a higher number of regions that are in contact with the image boundary, because the boundary of an image is not considered to be a region border. Merging a high number of regions in contact with the image boundary is not desirable. Eventually, R_{ik} sets with the metric $m_{R_{ik}}$ higher than 0 are removed, because the metric $m_{R_{ik}}$ corresponds with the value $grd_\alpha(x,y)$ of border pixels with correct direction α, which are assumed to have negative values. The resulting mask of a matrix determining the satisfactory sets R_{ik} is shown in Fig. 7d. As can be seen, many of the sets R_{ik} are filtered out. Further, it is good to point out that the sets R_{ik} can be identical for different i, see Fig. 7a,b,c, where merging procedures with different initial regions R_i can end up with identical sets R_{ik} (the metrics have the same values). At this point, duplicate sets R_{ik} are removed and a list of the remaining unique sets R_{ik} is created. The number of sets on the list is reduced and the best set is selected during the following steps.

1. 50% of sets R_{ik} with the highest metric $s_{R_{ik}}$ are removed from the list.

2. 50% of sets R_{ik} with the lowest metric $c_{R_{ik}}$ are removed from the list reduced in the previous step.

3. 50% of sets R_{ik} with the highest metric $m_{R_{ik}}$ are removed from the list reduced in the previous step.

4. The set R_{ik} with the highest metric $c_{R_{ik}}$ is selected.

This way the list of suitable sets of R_{ik} is reduced from different perspectives and the set R_{ik} which best represents the resulting segment is selected, see Fig. 8a. The regions of R_{ik} can be easily connected via morphological closing, see Fig. 8b. After this stage the grain is identified in the image.
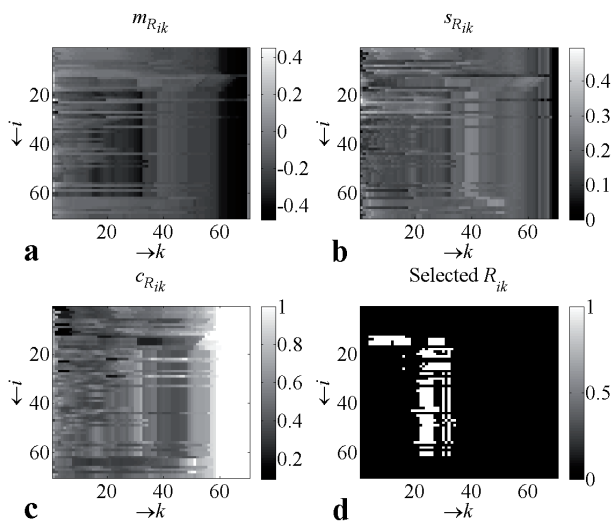

Fig. 7. Visualization of matrices, (a) **M**, (b) **S**, (c) **C**, (d) mask determining promising sets of regions.

2.6 Boundary Refining

As stated before, steerable filters are used in order to extract significant intensity changes while suppressing intensity changes of texture and noise. However, this procedure can cause a deviation in edge position and thus also a boundary deviation of the resulting segment. For segment extraction with a more precise position of boundaries, watershed segmentation can be used once again. The gradient magnitude image $grd_{abs}(x,y)$ is determined as the sum of absolute values of images filtered in two mutually perpendicular directions, similarly to (1), but now the Sobel filter is used instead of the steerable filter. The Sobel filter is designed for edge detection without noise suppression, thus it gives more precise results. In comparison with watershed segmentation as used in the initial stage, the position, shape and size of grain are now fairly well known, which can be exploited for creating markers for marker-controlled segmentation. A marker image contains only two markers for the grain and background, where the background marker is simply set as the boundaries of image, the grain marker object is obtained by reducing the resulting segment from the previous stage, e.g. by applying morphological erosion with the structuring element of a suitable size, see marker

image in Fig. 8c. Using this marker image, the initial points of flooding for the watershed transform are set and segmentation is performed, resulting in the final extraction of grain mask, see Fig. 8d.
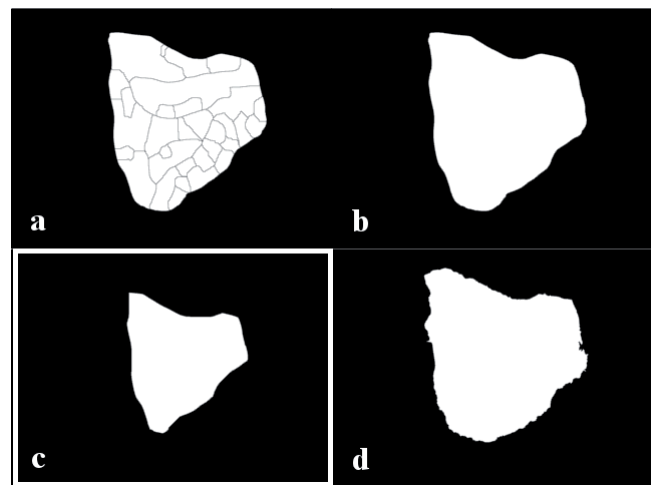

Fig. 8. (a) Set of regions selected after region merging stage. (b) Resulting segment after region merging stage. (c) Marker image. (d) Resulting mask after boundary refining.

3. Experimental Results

The proposed algorithm was tested on an available database of 340 images. For the evaluation of segmentation results the ground-truth masks of grains from the database were used. Image resolution was left at its original value 1280 x 960 pixels.

3.1 Optimal Parameter of Watershed Splitting Stage

First, the accuracy of splitting into regions using the watershed transform was evaluated with respect to the parameter t_{mark} of gradient image thresholding. The assumption for the method giving a correct segment in region merging is that the borders of the ground-truth mask overlap with the borders of some regions. Thus, to evaluate whether watershed splitting can be used, the percentage of ground-truth mask border pixels intersected by border pixels of regions was examined. Region borders were thickened via morphological dilation in order to introduce a degree of tolerance when the border pixel of ground-truth mask is close to some border pixel of regions so that the ground-truth mask pixel can be considered intersected. The results of watershed splitting are influenced by the threshold t_{mark}, which is used for the extraction of markers, see Fig. 4c. Markers are determined as connected components after thresholding the image $grd_{abs}(x,y)$. If t_{mark} is too high, a lower number of bigger markers is obtained and this can cause that a correct segment cannot be merged from the regions created, see Fig. 9a. On the other side, too many small markers are extracted when the t_{mark} used is too low,

see Fig. 9b. To take into account different value distributions of $grd_{abs}(x,y)$, x-th percentile of $grd_{abs}(x,y)$ histogram was selected as the threshold t_{mark} for every image, which means that the same total area of image belongs to markers in case of every image. Plotted in Fig. 10 is the average percentage (together with the standard deviation) of intersected border pixels of mask depending on the x parameter of the x-th percentile as well as the average number of regions depending on x. As can be seen, the 35-th percentile of $grd_{abs}(x,y)$ histogram can be considered as the optimal value, because the value of average percentage (together with the standard deviation) is not getting better with x-values lower than 35, but the average number of regions is still getting higher. The result of splitting for $x = 35$ is shown in Fig. 9c.
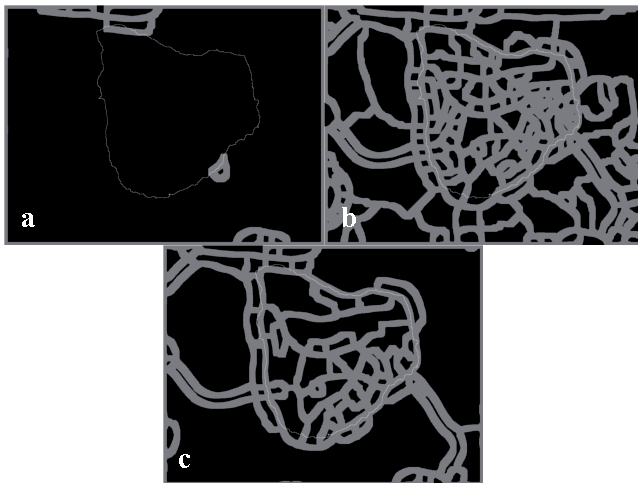

Fig. 10. Influence of threshold t_{mark} on average percentage of intersections (together with standard deviation) and average number of regions. Threshold t_{mark} is given as the x-th percentile of $grd_{abs}(x,y)$ histogram.

Fig. 9. Splitting into regions, (a) t_{mark} too high, (b) t_{mark} too low, (c) optimal t_{mark}.

3.2 Segmentation Results Evaluation

The evaluation of the total results of the proposed method was carried out by comparing the automatically determined segment with the ground-truth mask. The resulting segment overlaps with the mask; pixel numbers denoted as *TP* (True Positives), *FP* (False Positives), *FN* (False Negatives), and *TN* (True Negatives) are computed. Using these numbers, precision = $TP/(TP+TN)$ and recall = $TP/(TP+FN)$ are evaluated. If the precision value is less than 100%, than a particular part of the segment area is incorrectly marked as grain area, see Fig. 11a,b. If the recall value is less than 100%, some part of the segment area is incorrectly marked as background, see Fig. 11c,d.

Fig. 12 presents the results after the region merging stage, when the segment is determined by the selected set of regions R_{ik}; the vertical axis represents the percentage of testing images, whose precision or recall is equal to or higher than the value on the horizontal axis. The specific values from the graphs can be seen in Tab. 1. Obviously, the proposed method produces encouraging results. For example, if precision and recall values of 95% are allowed, then these requirements are fulfilled for 86.2% and 71.2%
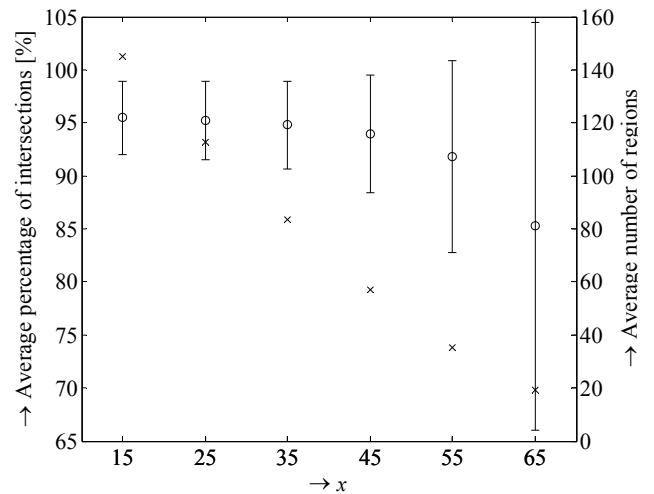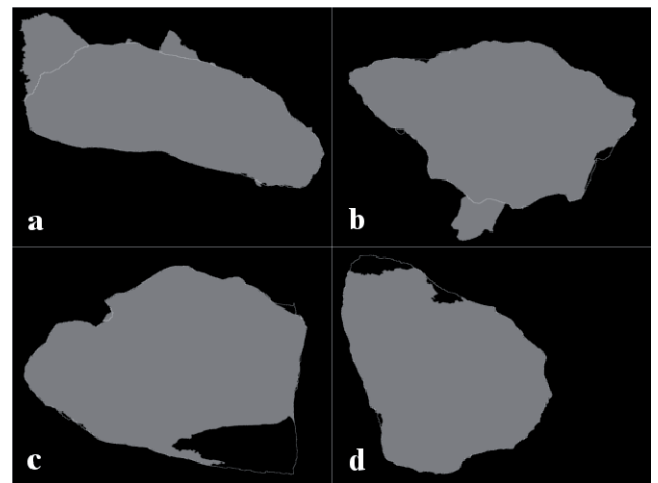

Fig. 11. Examples of evaluated segmentation results, (a) precision = 90%, (b) precision = 95%, (c) recall = 90%, (d) recall = 95%.

of images in the testing database, respectively. If precision and recall values of 90% are allowed, then these requirements are fulfilled for 96.2% and 82.1% of images in the testing database, respectively. This implies that the proposed method reaches better results from the viewpoint of precision, which is desirable from the perspective of further usage of the extracted segments, because parts of background included in further processing of grain texture statistics could cause errors; conversely, small parts of grain not included in further processing are not critical.

After the stage of boundary refining, when watershed segmentation is applied to the $grd_{abs}(x,y)$ image obtained using the Sobel filters, the results of segmentation are further improved due to the more accurate positions of the segment borders, see Fig. 13 and Tab. 2. If precision and recall values of 95% are allowed, then these requirements are fulfilled for 96.2% and 82.9% of images in the testing database, respectively. If precision and recall value of 90%

are allowed, then these requirements are fulfilled for 97.6% and 95.0% of images in the testing database, respectively. After the stage of boundary refining, the average value of precision is 98.5%, the average value of recall is 96.1%.
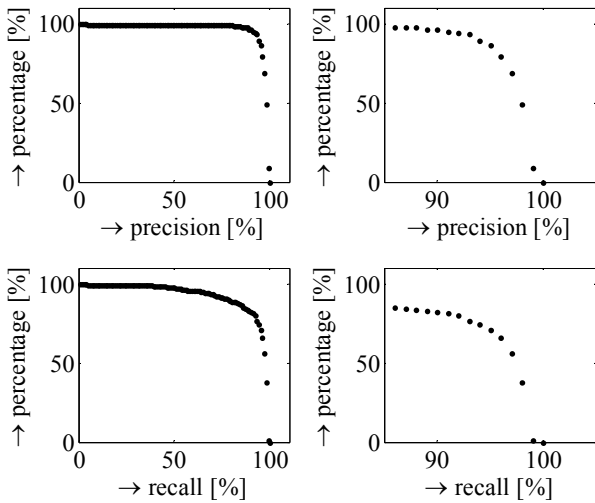

Fig. 12. Results after stage of region merging, vertical axes represent percentage of image database which was successfully segmented with precision/recall value on horizontal axes, plots on the right are detailed versions of plots on the left.

Precis. [%]	Perc. [%]	Precis. [%]	Perc [%]	Recall [%]	Perc. [%]	Recall [%]	Perc. [%]
100	0.0	93	93.2	100	0.0	93	76.8
99	8.8	92	94.1	99	1.2	92	80.0
98	48.8	91	95.0	98	37.6	91	81.2
97	68.5	90	96.2	97	56.2	90	82.1
96	79.1	85	97.9	96	66.2	85	86.2
95	86.2	80	98.8	95	71.2	80	88.8
94	89.1	75	98.8	94	74.1	75	91.2

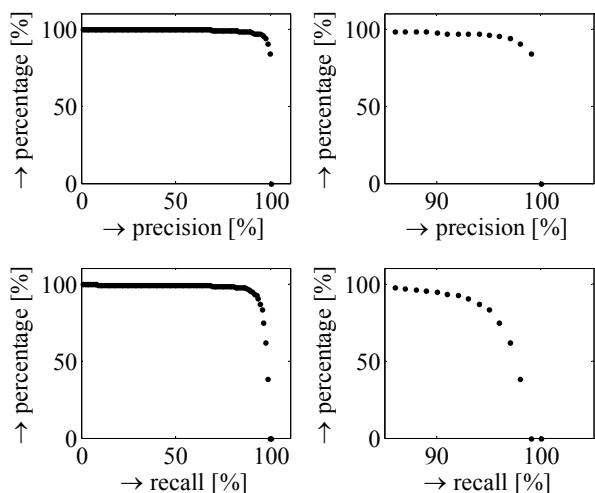**Tab. 1.** Results after stage of region merging.

Fig. 13. Results after stage of boundary refining, vertical axes represent percentage of image database which was successfully segmented with precision/recall value on horizontal axes, plots on the right are detailed versions of plots on the left.

Precis. [%]	Perc. [%]	Precis. [%]	Perc. [%]	Recall [%]	Perc. [%]	Recall [%]	Perc. [%]
100	0.0	93	97.1	100	0.0	93	90.6
99	83.8	92	97.1	99	0.0	92	92.6
98	90.6	91	97.1	98	38.5	91	92.9
97	93.8	90	97.6	97	61.5	90	95.0
96	95.3	85	98.2	96	74.4	85	97.4
95	96.2	80	98.8	95	82.9	80	97.9
94	96.8	75	99.1	94	86.8	75	97.9

Tab. 2. Results after stage of boundary refining.

4. Conclusion

In this work, the segmentation of sedimentary grain in electron microscopy images was investigated. Commonly used segmentation techniques are not sufficient for the segmentation of such complex images, thus a novel method for the specific case of sedimentary grains was developed and tested. The principle of the method is based on the common characteristic properties of grains, i.e. typical intensity changes on grain borders and compact shape. Using these properties, specialized evaluation metrics were proposed for determining the segments correctly.

The resulting segment is supposed to be used as an area from which various textural features are extracted and which is examined to reveal typical structure forms. From this perspective, it can be concluded that experimental results of the proposed method are very good. Specifically, the average precision after the stage of boundary refining is 98.5%. This means that in a minor number of cases, a significant part of image belonging to the background is labeled as the grain part. This property of algorithm is very advantageous because in further texture processing it is less probable that typical features will be extracted also from the background image parts, which could negatively influence the feature values obtained. The average recall value after the stage of boundary refining is 96.1%, which is a lower value than the precision value; however, it is still a very positive result. Moreover, when a small part of grain is not available for the next processing, it is an insignificant problem, because the correctly segmented major part of the grain can be considered as sufficiently representing the texture properties. The next research will be aimed at investigating the characteristics which can be extracted using a computer and which are the most discriminating from the viewpoint of distinguishing between geomorphological geneses.

Acknowledgements

References

[1] KŘÍŽOVÁ, L., KŘÍŽEK, M., LISÁ, L. Applicability of quartz grains surface analysis to the study of the genesis of unlithified sediments. *Geografie*, 2011, vol. 116, no. 1, p. 59–78.

[2] WESZKA, J. S. A survey of threshold selection techniques. *Computer Graphics and Image Processing*, 1978, vol. 7, no. 2, p. 259–265.

[3] OTSU, N. A threshold selection method from gray-level histograms. *IEEE Transactions on Systems, Man and Cybernetics*, 1979, vol. 9, no. 1, p. 62–66.

[4] RIDDLER, T. W., CALVARD, S. Picture thresholding using an iterative selection method. *IEEE Transactions on Systems, Man and Cybernetics*, 1978, vol. 8, no. 8, p. 630–632.

[5] CANNY, J. A computational approach to edge detection. *IEEE Transactions Pattern Analysis and Machine Intelligence*, 1986, vol. 8, no. 6, p. 679–698.

[6] PRAGER, J. Extracting and labeling boundary segments in natural scenes. *IEEE Transactions on Pattern Analysis and Machine Intelligence*, 1980, vol. 2, no. 1, p. 16–27.

[7] BEUCHER, S., LANTUEJOUL, C. Use of watersheds in contour detection. In *International Workshop on Image Processing, Real-Time Edge and Motion Detection*, 1979.

[8] VINCENT, L., SOILLE, P. Watersheds in digital spaces: an efficient algorithm based on immersion simulations. *IEEE Transactions on Pattern Analysis and Machine Intelligence*, 1991, vol. 13, no. 6, p. 583–598.

[9] MEYER, F. Topographic distance and watershed lines. *Signal Processing*, 1994, vol. 38, no. 1, p. 113–125.

[10] VINCENT, L. Morphological grayscale reconstruction in image analysis: Applications and efficient algorithms. *IEEE Transactions on Image Processing*, 1993, vol. 2, no. 2, p. 176–201.

[11] GRAU, V., MEWES, U. J., ALCAÑIZ, M., KIKINIS, R., WARFIELD, S. K. Improved watershed transform for medical image segmentation using prior information. *IEEE Transactions on Medical Imaging*, 2004, vol. 23, no. 4, p. 447–458.

[12] FRUCCI, M., RAMELLA, G., SANNITI DI BAJA, G. Using resolution pyramids for watershed image segmentation. *Image and Vision Computing*, 2007, vol. 25, no. 6, p. 1021–1031.

[13] BRICE, C. R., FENNEMA, C. L. Scene analysis using regions. *Artificial Intelligence*, 1970, vol. 1, no. 3-4, p. 205–226.

[14] CHANG, Y., LI, X. Adaptive image region-growing. *IEEE Transactions on Image Processing*, 1994, vol. 3, no. 6, p. 868-872.

[15] NOCK, R., NIELSEN, F. Statistical region merging. *IEEE Transactions on Pattern Analysis and Machine Intelligence*, 2004, vol. 26, no. 11, p. 1452–1458.

[16] HORROWITZ, S. L., PAVLIDIS, T. Picture segmentation by a tree traversal algorithm. *Journal of the Association for Computing Machinery*, 1976, vol. 23, no. 2, p. 368–388.

[17] HARIS, K., EFSTRATIADIS, S. N., MAGLAVERAS, N., KATSAGGELOS, K. Hybrid image segmentation using watersheds and fast region merging. *IEEE Transactions on Image Processing*, 1998, vol. 7, no. 12, p. 1684–1699.

[18] BEIL, M., IRINOPOULOU, T., VASSY, J., WOLF, G. A dual approach to structural texture analysis in microscopic cell images. *Computer Methods and Programs in Biomedicine*, 1995, vol. 48, no. 3, p. 211–219.

[19] KORTING, T. S., DUTRA, L. V., FONSECA, L. M. G. A resegmentation approach for detecting rectangular objects in high-resolution imagery. *IEEE Geoscience and Remote Sensing Letters*, 2011, vol. 8, no. 4, p. 621–625.

[20] LUMBRERAS, F., SERRAT, J. Segmentation of petrographical images of marbles. *Computers & Geosciences*, 1996, vol. 22, no. 5, p. 547–558.

[21] HAMARNEH, G., LI, X. Watershed segmentation using prior shape and appearance knowledge. *Image and Vision Computing*, 2009, vol. 27, no. 1-2, p. 59–68.

[22] CHEVREFILS, C., CHERIET, F., AUBIN, C. E., GRIMARD, G. Texture analysis for automatic segmentation of intervertebral disks of scoliotic spines from MR images. *IEEE Transactions on Information Technology in Biomedicine*, 2009, vol. 13, no. 4, p. 608–620.

[23] ROUSSILLON, T., PIÉGAY, H., SIVIGNON, I., TOUGNE, L., LAVIGNE, F. Automatic computation of pebble roundness using digital imagery and discrete geometry. *Computers & Geosciences*, 2009, vol. 35, no. 10, p. 1992–2000.

[24] LU, B., CUI, M., LIU, Q., WANG, Y. Automated grain boundary detection using the level set method. *Computers & Geosciences*, 2009, vol. 35, no. 2, p. 267–275.

[25] BARRAUD, J. The use of watershed segmentation and GIS software for textural analysis of thin sections. *Computers & Geosciences*, 2006, vol. 154, no. 1-2, p. 17–33.

[26] MARTINEZ-SANCHEZ, A., GARCIA, I., FERNANDEZ, J. A ridge-based framework for segmentation of 3D electron microscopy datasets. *Journal of Structural Biology*, 2013, vol. 181, no. 1, p. 61–70.

[27] FRANGAKIS, A. S., HEGERL, R. Segmentation of two- and three-dimensional data from electron microscopy using eigenvector analysis. *Journal of Structural Biology*, 2002, vol. 138, no. 1-2, p. 105–113.

[28] FREEMAN, W. T., ADELSON, E. H. The design and use of steerable filters. *IEEE Transactions Pattern Analysis and Machine Intelligence*, 1991, vol. 13, no. 9, p. 891–906.

About Authors ...

Aleš KŘUPKA received his MSc degree in Electrical Engineering from Brno University of Technology in 2012. His research work is focused on image and video processing, especially image segmentation, object detection and information extraction from image objects.

Kamil ŘÍHA received his M.Sc. degree in Electronics & Communication in 2003 and the Ph.D. degree in 3D Scene Acquisition for Auto-Stereoscopic Display in 2007. Presently, he is employed at Brno University of Technology, Faculty of Electrical Engineering, Department of Telecommunications, as the academic employee (since 2006). His research interests include in particular areas of digital image and video processing

Lenka KŘÍŽOVÁ received her M.Sc. degree in Physical Geography and Geoecology at Charles University in Prague in 2010. Her research in geomorphology field focuses on the micromorphology of quartz grains, drawing on connections to paleogeography.